Interference Effect on the Performance of Fingerprinting Localization

Arash Behboodi*, Filip Lemic†, Adam Wolisz†, Rudolf Mathar*
†Institute for Theoretical Information Technology, RWTH Aachen University
†Telecommunication Networks Group (TKN), Technische Universität Berlin
Email: {arash.behboodi,mathar}@ti.rwth-aachen.de, {lemic,wolisz}@tkn.tu-berlin.de

***Abstract*—With the abundance of mobile connected devices and coexisting networks, localization solutions are inevitably subject to interference. In this paper, effects of interference on the performance of Fingerprinting Localization Algorithms (FPS) are studied both theoretically and through experimentation. The previously introduced theoretical framework based on Hypothesis Testing (HT) problem is employed to characterize the performance of FPS and provide guidelines for combating negative impact of interference. In particular, it is shown that background interference interestingly can improve the performance of FPS, while the interference in the measurement phase incurs an error by pushing the reported location closer to the anchors. Moreover, the anchors provide the highest interference robustness for locations in their proximity. These results are further verified through simulations and experimentation in realistic setups.**

I. Introduction

Location information is an indispensable requirement for providing context-aware services, location-aware and pervasive computing, ambient intelligence, and location-based services. Significant efforts have been invested in developing localization solutions that can, both indoor and outdoor, provide locations of objects and individuals with precision and accuracy required by the target application. It is more favorable for localization solutions to leverage available technologies and infrastructures and hence avoid extra hardware development and deployment costs. In that regard, Radio-Frequency (RF)-based solutions that utilize technologies such as IEEE 802.11 (WiFi), IEEE 802.15.4 (ZigBee), IEEE 802.15 (Bluetooth), Ultra-Wide Band (UWB), RFID, and mobile networks are particularly interesting.

However, as the density of wireless devices increases, wireless networks and services are more subject to unintended wireless transmissions from other devices. Interference turns out to be a bottleneck for many wireless networks by reducing the Signal to Interference Noise Ratio (SINR). Many research pieces attempted to address interference problem by devising different techniques for interference avoidance, cancellation, and coordination [1]–[3]. However, it is much more difficult and much less attempted to characterize the effects of interference on localization solutions. In general, localization solutions are complex systems influenced by infrastructure, used technology, signal processing algorithms, and propagation environment. The effect of interference is the aggregation of its effects on each part of the system. Even the same type of interference can have dissimilar effects on different technologies (IEEE 802.11, IEEE 802.15.4, etc.) and on the localization parameters reported by each technology.

978-1-5090-6299-7/17/$31.00

In this work, we focus on Received Signal Strength (RSS)-based fingerprinting solutions, one of the most promising approaches for indoor indoor localization. Different aspects of fingerprinting algorithms have been studied vastly in the literature [4]–[8]. The main theoretical work on fingerprinting algorithms is [9], where the authors provide an analysis of the effect of the number of visible Access Points (APs) and radio propagation parameters on the performance of fingerprinting algorithms. These results are extended to complexity analysis in [10]. The authors in [11] proposed a probabilistic model for RSS-based fingerprinting relating locations to received RSS. The performance of fingerprinting algorithms has then been discussed using likelihood-based detection algorithms and insights have been provided for fingerprinting design.

The general belief is that the interference between APs degrades the performance of localization solutions [12]. In WiFi-based systems one effect of interference is the loss of beacon packets, which impacts harmfully Received Signal Strength Indicator (RSSI)-based fingerprinting algorithms [13]. However, if the packet is correctly received, the interference can still affect RSSI values. Based on a set of measurements using telosB with a CC2420 radio, it has been observed that the interference effect on RSSI values is additive [14] (and a similar work in [15]). This idea has been explored experimentally and theoretically in [16], where the effect of interference on packet-based RSSI, reported by IEEE 802.11 and IEEE 802.15.4 technologies, and on the Time of Flight (ToF) measured by IEEE 802.15.4 nodes was studied. From an information theoretic perspective three regimes have been identified. With low interference power, no significant changes are observed in RSSI values. When the interference power increases and passes a certain threshold, the RSSI value start to change and afterward they change almost linearly with the interference power in dBm until a certain threshold where packet reception is no longer possible. Note that in general the interference power is added to the received power when measured in Watt and not dBm.

In this work, we employ the theoretical framework developed in [17], [18] to study the effect of interference on RSS-based fingerprinting algorithms. The signal feature is assumed to be the RSS value. It is assumed that RSS values are measured in Watt and not obtained from beacon packets. Therefore, the main effect of interference is changing the

RSS values and not the packet loss. The variation due to interference is modeled by an additive term. Based on [17], a function based on Kullback-Leibler (KL)-divergence is used as the performance metric encapsulating both latency and accuracy. It is shown that the interference, if it is present in both training and measurement phases, can improve the performance of fingerprinting solutions for a part of the region. On the other hand, if the interference is only present in the measurement phase, the localization solution tends, for a location in proximity to interference, to "push" the position estimate closer to the anchors. These results are supported by both theoretical and numerical investigations.

The paper is organized as follows. In section II, the system model is introduced including propagation channel and RSS model. The interference effect on localization solutions are discussed theoretically in section III. The experimental and analytical evaluations are given in Section IV.

II. System Model

The localization system consists of K dedicated anchors used for localization. The location of the anchor i and the target node are respectively given by $\mathbf{w}_i$ and $\mathbf{u}$ both in an Euclidean space $\mathbb{R}^d$. The anchor i's signal is denoted by $x^{(i)}(t)$ with transmission power $P_T^{(i)}$. The received signal from the anchor i can be modeled as follows [19]:

$$y^{(i)}(\mathbf{u},t) = \sum a_j^{(i)}(t) x^{(i)}(t-\tau_j^{(i)}(t)) + z^{(i)}(t), \qquad (1)$$

where $a_j^{(i)}(t)$ and $\tau_j^{(i)}(t)$ are the channel gain and delay of j'th multi-path component. The fingerprint at the point $\mathbf{u}$ is then $\mathbf{X_u} = (X_{\mathbf{u}}^{(1)}, \ldots, X_{\mathbf{u}}^{(K)})$ where $X_{\mathbf{u}}^{(i)}$ is the fingerprint of the anchor i which is supposed to be the received power $P^{(i)}(\mathbf{u})$. In this work, it is assumed that the received power is calculated over long period and therefore the small scale fading is averaged out. Moreover assuming one dominant channel tap, the attenuation is assumed to be proportional to $\frac{1}{\|\mathbf{w}_i-\mathbf{u}\|^{\alpha/2}}$ with α is the path loss exponent, assumed to be the same for all the anchors. For example, WiFi RSSI values vary only slightly in time and that mainly due to quantization noise. Therefore the fingerprint $X_{\mathbf{u}}^{(i)}$ writes as:

$$X_{\mathbf{u}}^{(i)} = P^{(i)}(\mathbf{u}) = \frac{P_T^{(i)}}{\|\mathbf{w}_i-\mathbf{u}\|^{\alpha}} + N + \mathbf{N}_i, \qquad (2)$$

where N is the additive noise power, $\mathbf{N}_i$ is a Gaussian random variable of variance N_i to account for small changes in RSS values. Suppose that the interference is present at $\mathbf{w}_I$ and is transmitting with power P_I. The total received power now has an additive interference part. The new fingerprints under this condition are given by:

$$X_{\mathbf{u}}^{(i)} = P^{(i)}(\mathbf{u}) = \frac{P_T^{(i)}}{\|\mathbf{w}_i-\mathbf{u}\|^{\alpha}} + \frac{P_I}{\|\mathbf{w}_I-\mathbf{u}\|^{\alpha}} + N + \mathbf{N}_i. \qquad (3)$$

III. Interference Effect on Fingerprinting

To analyze the effect of interference on performance of fingerprinting localization solutions, we adopt the framework introduced in [18]. In the framework, it was assumed that the measured feature for localization is probabilistically related to the measurement location and the relation is characterized through a probability distribution function. The localization problem is recognized as hypothesis testing problem for the probability distribution of the measured feature at each location. Indeed, it has been shown in [18] that knowing the probability distribution and with some mild conditions, one can accurately localize each object with sufficient number of measurements. Kullback-Leibler (KL) divergence measures the difference between probability distributions and appears as a central performance metric. In general, the smaller the KL divergence of the probability distributions at two different locations, more measurements are needed to distinguish them, and hence higher latency. Therefore, KL divergence is used in this work as the metric to evaluate the latency and accuracy of underlying localization solution under interference.

A. Interference in Training and Measurement Phase

In this section, it is assumed that interference is present in both training and measurement phases. The probability distributions of the feature at two locations $\mathbf{u}_1$ and $\mathbf{u}_2$ is given by $\mathbb{P}_{\mathbf{X}|\mathbf{u}_1}$ and $\mathbb{P}_{\mathbf{X}|\mathbf{u}_2}$ characterized by (2) and (3). It is known from [17], [18] that the accurate localization is possible in this case under sufficient number of measurements and training points. KL-divergence is used to evaluate the performance of localization solutions. For the case where no interference is present, the KL-divergence is evaluated as:

$$D(\mathbb{P}_{\mathbf{X}|\mathbf{u}_1}\|\mathbb{P}_{\mathbf{X}|\mathbf{u}_2}) = \sum_j \frac{(P_T^{(j)})^2}{2N_j}\left(\frac{1}{\|\mathbf{w}_j-\mathbf{u}_1\|^{\alpha}} - \frac{1}{\|\mathbf{w}_j-\mathbf{u}_2\|^{\alpha}}\right)^2. \qquad (4)$$

On the other hand, when the interference is there, the new KL-divergence $D(\mathbb{P}^I_{\mathbf{X}|\mathbf{u}_1}\|\mathbb{P}^I_{\mathbf{X}|\mathbf{u}_2})$ is given by:

$$D(\mathbb{P}^I_{\mathbf{X}|\mathbf{u}_1}\|\mathbb{P}^I_{\mathbf{X}|\mathbf{u}_2}) = \sum_j \frac{1}{2N_j}\left(\frac{(P_T^{(j)})^2}{\|\mathbf{w}_j-\mathbf{u}_1\|^{\alpha}} - \frac{(P_T^{(j)})^2}{\|\mathbf{w}_j-\mathbf{u}_2\|^{\alpha}} + \frac{P_I^2}{\|\mathbf{w}_I-\mathbf{u}_1\|^{\alpha}} - \frac{P_I^2}{\|\mathbf{w}_I-\mathbf{u}_2\|^{\alpha}}\right)^2. \qquad (5)$$

Similar to [18], the previous expressions are evaluated for the case $D(\mathbb{P}_{\mathbf{X}|\mathbf{u}}\|\mathbb{P}_{\mathbf{X}|\mathbf{u}+\mathbf{e}})$ which indicates how well two points of distance $\|e\|$ can be distinguished as a function of $\mathbf{u}$ and system parameters. The functions $\ell(\mathbf{u},\mathbf{e}) = D(\mathbb{P}_{\mathbf{X}|\mathbf{u}}\|\mathbb{P}_{\mathbf{X}|\mathbf{u}+\mathbf{e}})$ and $\ell_I(\mathbf{u},\mathbf{e}) = D(\mathbb{P}^I_{\mathbf{X}|\mathbf{u}}\|\mathbb{P}^I_{\mathbf{X}|\mathbf{u}+\mathbf{e}})$ are called *resolvability functions* since they indicated how well one can resolve two points of fixed distance. As expected, if $\mathbf{u}$ is far from the interference, then the interference does not have a major effect. This is different for those points close to the interference. Interestingly, $\ell_I(\mathbf{u},\mathbf{e})$ is very large for points closer to the interference source, compared to the case where no interference is present. With background interference, the

points closer to the interferer can be better distinguished from their neighbors of distance $\|\mathbf{e}\|$. This means that the accuracy and latency features of localization for those points are significantly improved. This can be seen in Figure 1 where two cases are compared. At first no interference is present, followed by the case when fingerprinting is done with a background interference. All sources have unit power, path-loss exponent is 2, and $\mathbf{e} = (0.1, 0.1)$ with meter as the unit in an area of $3 \times 3m^2$. The level curves of $\ell_I(\mathbf{u}, \mathbf{e})$ and $\ell(\mathbf{u}, \mathbf{e})$ are shown with same values attributed to the same color. Note that the KL-divergence is significantly improved around the interferer's location meaning that interference can actually improve fingerprinting localization performance for points close to the interferer's source. Another hint from this discussion pertains to anchor placement. If the positions of background interference are known, one can deploy dedicated localization anchors more efficiently by placing them far from interference sources.

B. Interference in Measurement Phase

Consider the case where the interference is only present in the measurement phase and not the training phase. In this case, interference changes the fingerprints such that the closest fingerprint to the one measured under interference might not be any more the fingerprint taken at that location. When the interference is not present, at a given location, the KL-divergence between feature probability distributions in the training and measurement phases is trivially zero since they both have the same statistics. This is not the case when interference is present. Suppose that the feature probability distribution at $\mathbf{u}_1$ in the measurement phase is given by $\mathbb{P}^I_{\mathbf{X}|\mathbf{u}_1}$. To see how much interference corrupts the fingerprint distribution, consider the probability distribution in the training set which is the most similar one to $\mathbb{P}^I_{\mathbf{X}|\mathbf{u}_1}$:

$$\hat{\mathbf{u}}_1 = \arg\min_{\mathbf{u}} D(\mathbb{P}_{\mathbf{X}|\mathbf{u}} \| \mathbb{P}^I_{\mathbf{X}|\mathbf{u}_1}), \tag{6}$$

This implies an error $\|\hat{\mathbf{u}}_1 - \mathbf{u}_1\|$. When no interference is present, this error will be zero. To get some intuition about how big the error can get under interference, consider the function $\ell_{\mathbf{u}_1}(\mathbf{u}) = D(\mathbb{P}_{\mathbf{X}|\mathbf{u}} \| \mathbb{P}^I_{\mathbf{X}|\mathbf{u}_1})$. We call it *the identification function* at $\mathbf{u}_1$ because it shows how well one can identify the location $\mathbf{u}_1$ in the measurement phase. The level curves of this function indicate how well different points in the space are distinguishable from $\mathbf{u}_1$. In idea situation, the function is minimized at $\mathbf{u}_1$ and rapidly increases by moving away from the point. The maximum value of this function is then attained around the anchors, which is expected given that points closer to the anchors have better accuracy. Under interference these level curves are displaced. Following theorem is a hint on how the level curves are deformed.

Theorem 3.1: Consider a fingerprinting localization solution composed of K anchors placed at $\mathbf{w}_1, \ldots, \mathbf{w}_K$ and an interference source at $\mathbf{w}_I$.

1) Under interference, the reported location is either the same or closer to at least one anchor compared to the actual location.
2) Suppose that the interference source is outside the convex hull[1] of anchors and suppose that $\mathbf{u}_1$ is a point outside the convex hull of anchors and in proximity of the interference source. Then the estimated location $\hat{\mathbf{u}}_1$ by KL-divergence based FPS belongs to the convex hull of anchors.

Proof: As for the first part of the theorem, for the simple model introduced above, the function $\ell_{\mathbf{u}_1}(\mathbf{u})$ is characterized as follows:

$$\ell_{\mathbf{u}_1}(\mathbf{u}) = \sum_j \frac{1}{2N_j} \left(\frac{(P_T^{(j)})^2}{\|\mathbf{w}_j - \mathbf{u}_1\|^\alpha} - \frac{(P_T^{(j)})^2}{\|\mathbf{w}_j - \mathbf{u}\|^\alpha} + \frac{P_I^2}{\|\mathbf{w}_I - \mathbf{u}_1\|^\alpha} \right)^2. \tag{7}$$

For a fixed $\mathbf{u}_1$, the interference increases each fingerprint by $\frac{P_I^2}{\|\mathbf{w}_I - \mathbf{u}_1\|^\alpha}$. The reported location $\mathbf{u}^\star$ is the one attaining the minimum in (6). If this point $\mathbf{u}^\star$ is different from $\mathbf{u}_1$, then at least for one j, we should have $\|\mathbf{w}_j - \mathbf{u}_1\| \geq \|\mathbf{w}_j - \mathbf{u}^\star\|$. Otherwise we have:

$$\frac{(P_T^{(j)})^2}{\|\mathbf{w}_j - \mathbf{u}_1\|^\alpha} - \frac{(P_T^{(j)})^2}{\|\mathbf{w}_j - \mathbf{u}^\star\|^\alpha} > 0. \tag{8}$$

This means instead that $\ell_{\mathbf{u}_1}(\mathbf{u}^\star) > \ell_{\mathbf{u}_1}(\mathbf{u}_1)$ which is in contradiction with assumption of $\mathbf{u}^\star$ being the minimizer of (6). For the second part, assume that all powers are put equal to one. If $\mathbf{u}^\star$ is the minimizer in (6), then it should satisfy the following gradient constraints:

$$\nabla_{\mathbf{u}} \ell_{\mathbf{u}_1}(\mathbf{u}) = 0, \tag{9}$$

which after standard manipulation leads to:

$$\sum_j \beta_j(\mathbf{u}, \mathbf{u}_1)(\mathbf{u} - \mathbf{w}_j) = 0, \tag{10}$$

with:

$$\beta_j(\mathbf{u}, \mathbf{u}_1) = \left(\frac{1}{\|\mathbf{w}_j - \mathbf{u}_1\|^\alpha} - \frac{1}{\|\mathbf{w}_j - \mathbf{u}\|^\alpha} + \frac{1}{\|\mathbf{w}_I - \mathbf{u}_1\|^\alpha} \right).$$

$\mathbf{u}^\star$ must satisfy this equation. If all $\beta_j(\mathbf{u}, \mathbf{u}_1)$'s are nonnegative or non-positive simultaneously with at least one of them non-zero, then the reported location belongs to the convex hull of anchors. In this sense, if a point is close to the interference source, i.e, if $\|\mathbf{w}_I - \mathbf{u}_1\|$ is very small, then $\beta_j(\mathbf{u}, \mathbf{u}_1)$'s are all positive and therefore $\mathbf{u}^\star$ is reported inside the convex hull of anchors. ■

The previous theorem can be examined from another perspective. First consider the following lemma.

Lemma 1: Suppose that $\mathbf{u}$ is in the convex hull of points $\mathbf{w}_1, \ldots, \mathbf{w}_K$. If for another point $\mathbf{v}$ we have:

$$\forall j \in \{1, \ldots, K\} : \|\mathbf{v} - \mathbf{w}_j\| \leq \|\mathbf{u} - \mathbf{w}_j\|, \tag{11}$$

then $\mathbf{v} = \mathbf{u}$.

Proof: From $\|\mathbf{v} - \mathbf{w}_j\| \leq \|\mathbf{u}_1 - \mathbf{w}_j\|$, it can be seen that:

$$\mathbf{v}^T\mathbf{v} + 2\mathbf{w}_j^T(\mathbf{u} - \mathbf{v}) \leq \mathbf{u}^T\mathbf{u}. \tag{12}$$

[1] A convex hull of a set X of points in a given space is the smallest convex set that contains X.

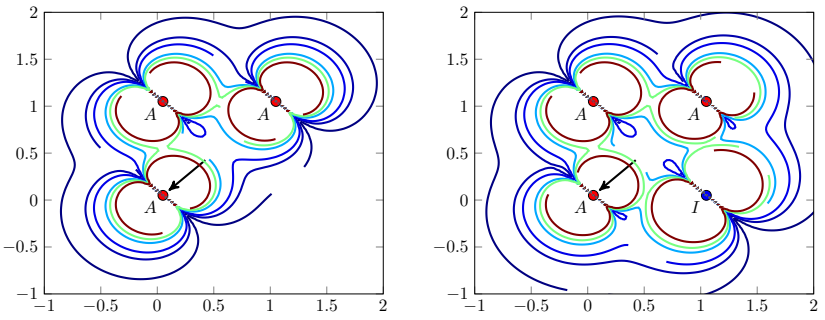

Fig. 1: Resolvability of points with distance 0.14m with 3 anchors (A) and 1 interference source (I) in $3 \times 3m^2$ - The arrow points toward increasing resolvability.

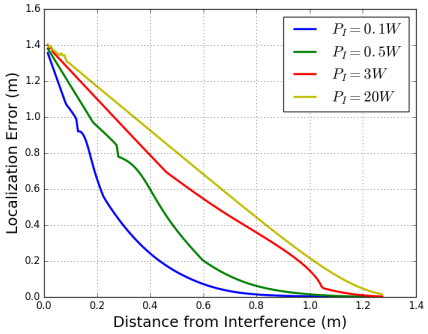

Fig. 2: Localization error versus distance from interference source for different interference powers

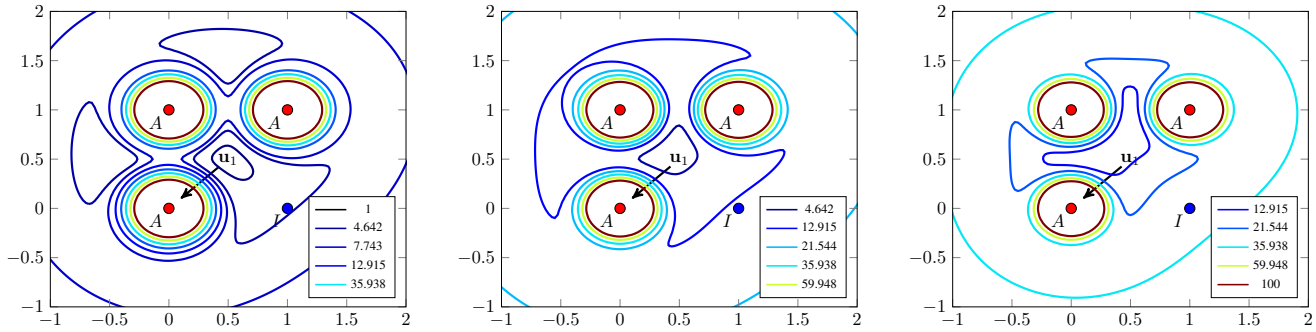

Fig. 3: Identification function for $\mathbf{u}_1$, $\ell_{\mathbf{u}_1}(\mathbf{u})$ for interference power $P_I = 0, 0.5$ and $1\ W$ in $3 \times 3m^2$

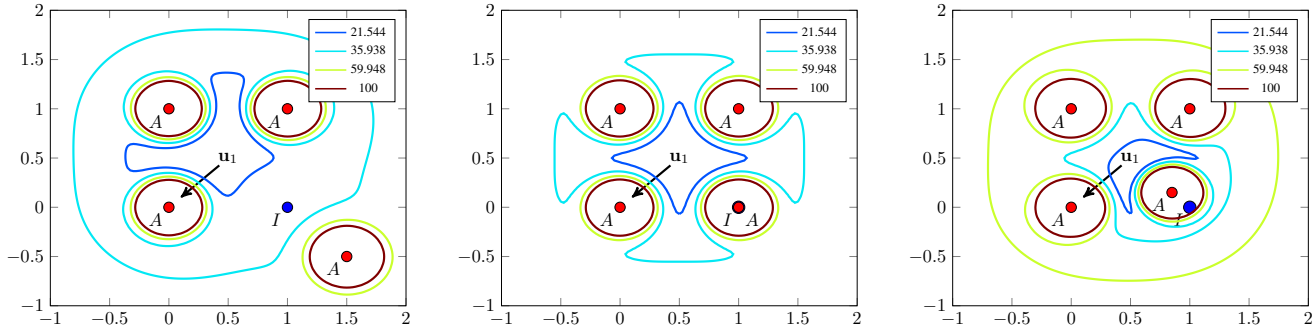

Fig. 4: Effect of anchor placement on $\ell_{\mathbf{u}_1}(\mathbf{u})$; anchors placed as $(0.5+\delta, 0.5-\delta)$ for $\delta = 1, 0.5, 0.35$

If $\mathbf{u}$ is in the convex hull of points $\mathbf{w}_1, \ldots, \mathbf{w}_K$, there are $\alpha_i \in [0,1]$ with $\sum \alpha_i = 1$ such that $\mathbf{u} = \sum \alpha_i \mathbf{w}_i$. Multiplying each inequality by α_i and summing up we have:

$$\sum_j \alpha_j \mathbf{v}^T\mathbf{v} + 2\sum_j \alpha_j \mathbf{w}_j^T(\mathbf{u}-\mathbf{v}) \le \sum_j \alpha_j \mathbf{u}^T\mathbf{u} \implies \mathbf{v}^T\mathbf{v} - 2\mathbf{u}^T\mathbf{v} + \mathbf{u}^T\mathbf{u} \le 0, \tag{13}$$

which means $\|\mathbf{v}-\mathbf{u}\| = 0$ and hence $\mathbf{v} = \mathbf{u}$. ■

Suppose that the actual location $\mathbf{u}_1$ is in the convex hull of anchors. If $\beta_j(\mathbf{u}^\star, \mathbf{u}_1) \le 0$ for all j, then the reported location is also inside the convex hull. But the negativity of $\beta_j(\mathbf{u}^\star, \mathbf{u}_1)$ implies that $\|\mathbf{u}^\star - \mathbf{w}_j\| \le \|\mathbf{u}_1 - \mathbf{w}_j\|$ for all j. An interesting implication of previous lemma is that $\mathbf{u}^\star$ should be equal to $\mathbf{u}_1$. But this is not be possible because $\beta_j(\mathbf{u}_1, \mathbf{u}_1)$ is positive. Therefore $\beta_j(\mathbf{u}^\star, \mathbf{u}_1)$ cannot all be non-positive. Note that the function $\beta_j(\mathbf{u}^\star, \mathbf{u}_1)$ shows how much interference pushes away the reported location from the actual one.

A very general rule of thumb is that the interference pushes the level curves of $\ell_{\mathbf{u}_1}(\mathbf{u})$ close to the anchors. Particularly those points close to the interference are affected severely by being pushed into the convex hull of anchors. This is expected because the interference is generally additive to the received power. By increasing the received power, it creates the appearance of receiving higher power and hence being close to the anchors. To see how the points closer to the interference are affected, consider the function $\ell_{\mathbf{u}_1}(\mathbf{u}_1)$, which boils down to $\|\mathbf{w}_I - \mathbf{u}_1\|^{-2\alpha}$. This expression shows how much interference corrupts the fingerprint at each point compared to the training phase. It is easy to see that the fingerprint corruption is inversely proportional to the distance to the interferer.

Figure 3 shows the level curves of $\ell_{\mathbf{u}_1}(\mathbf{u})$ with interference powers 0, 0.5 and 1. The anchors are denoted by the red points and have unit power, while the interferer is presented by a blue point. The arrow shows the direction of increase

in the values corresponding to level curves and same colors represent the same values in all figures. These figures present more intuitively the ideas discussed above regarding the effect of interference. Note that the error can be numerically characterized at each location by solving (6). In Figure 2 the error incurred by interference is found on each point located on the line from interference at (1,0) to the anchor at (0,1). It can be seen that the error decreases exponentially by distance from interference until it hits zero. By increasing the interference power, the decay of error by distance becomes linear.

C. Opportunistic Anchors for Interference Robustness

In the presence of the interferer, suppose that its location is available. Also suppose that the training phase is done using multiple anchors but only some of them are used in measurement phase and the rest are idle for example for energy efficiency purpose. The question is which anchor should be turned on to improve better the performance. An interesting question is to see whether it is always better to turn on an anchor close to the interferer.

In Figure 4 this scenario is discussed. In the figure, it can be seen that the anchor closer to the object of localization, and not necessarily closer to the interferer, provides better robustness. However, an anchor close to the interferer yields higher improvements in the overall performance of the system because the points closer to the interferer are subject to higher inaccuracies due to interference. On the other hand, if the localization of a specific object is desired, it is better to localize it in two steps. In the first step, existing infrastructure provides an approximate location of the object and in the second step, if needed, a new anchor close to the approximate location is activated to provide better accuracy.

IV. Evaluation

In this section, we demonstrate the consistency of the developed theory with the realistic behavior of fingerprinting algorithms under interference. First, we compare the results of the theory with the ones derived by leveraging a more complex model for indoor radio propagation. Second, we show the consistency of the theoretical results with the ones obtained through experimentation. As a fingerprint at each location, both for analytically and experimentally derived results, we use the vector of average RSS values observed from visible WiFi APs in a targeted environment, which is an often used signal feature in fingerprinting [20]. The pattern matching function between a fingerprint in the measurement phase and each fingerprint from the training phase is the Euclidean distance between RSS vectors, which is again an established method in indoor fingerprinting [21].

A. Analytical Evaluation

The footprint of the environment used in our simulation is given in Figure 5. The outer size of the environment is roughly 15x30 m^2. In the environment, we defined a set of four APs, with their transmission power set to 20 dBm and with their locations as indicated in the figure. We further defined a set of 40 training locations for fingerprinting, with their locations labeled with red dots in the figure. We modeled the RSS values from the four APs in each training location using the COST 231 multi-wall model for indoor radio propagation [22]. The model's applicability for indoor localization purposes has been demonstrated repeatedly (e.g. [17], [23], [24]). The model accounts for the type and number of walls and obstacles in an environment. The first attenuation contribution in the model is a one-slope term that relates the received power to distance. This attenuation contribution is characterized by the constant l_0 (the path-loss at 1 m distance from an AP and at the center frequency of 2.45 GHz) and the path-loss exponent α. Second, the number of walls in the direct path between an AP and a target location is counted and for each wall an attenuation contribution is assumed. The model yields RSS values from the defined APs at a target location.

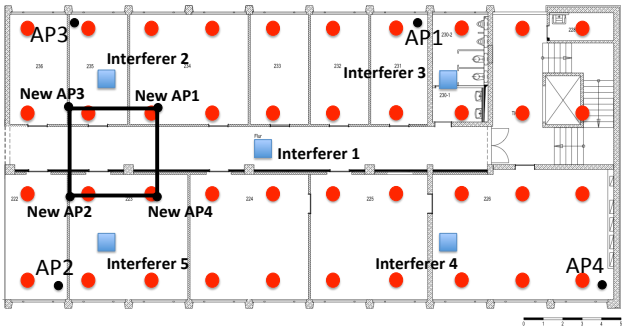

Fig. 5: Footprint of the environment used for deriving analytical results

In the parameterization of the model, we leveraged pre-collected measurements from the TWIST testbed environment with the same footprint [25] and used a least-square fitting procedure that allows minimizing the cost function between the measured received power and the modeled one. The parameters used as inputs to the model are the constant l_c related to the least-square fitting procedure, the path-loss exponent α, and the wall attenuation factor l_w. Moreover, a zero-mean Gaussian noise with standard deviation σ has been added to the obtained RSS values, which is a standard procedure in the simulation of the behavior of RSS-based localization systems [26], [27]. The procedure yielded the values for model parameter, i.e. l_c=53.73, α=1.64, and l_w=4.51. Furthermore, we defined σ=2 because similar variabilities of WiFi RSS measurements have been reported and usually used in the literature, e.g. [27], [28].

A target node's true location was selected randomly and the observed RSS values at that location were modeled using the outlined propagation model. By leveraging the modeled RSS values at the target node's location and the ones from the training locations as inputs to the selected fingerprinting algorithm, the target node's location was estimated. Furthermore, the localization error, i.e. the Euclidean distance between the estimated and the true location, was calculated. The procedure was repeated 10000 times and the results have been reported in a regular box-plot fashion.

First we evaluate the theoretical derived result claiming that, somewhat counterintuitive, if the interference is present in both phases of fingerprinting, the accuracy of fingerprinting can be improved. To evaluate this statement, in our simulation environment we introduced "Interferer 1", with its location as indicated in Figure 5. Interferer 1 is a source of constant interference. Using the previously discussed COST 231 model for radio propagation, the observed interference power due to Interferer 1 has been modeled at both training and evaluation locations. In the dB scale, interference has an additive effect on the observed RSS values from different APs, as discussed in [16]. In other words, in contrast to having no interference, if Interferer 1 is introduced in the environment, the observed RSS values from different APs at a given location are increased by the interference power observed at that location. Figure 6 compares the achieved fingerprinting accuracy in case there is no interference with the accuracies in case Interferer 1 is introduced, with different configurations of its transmit power. As visible in the figure, in case interference is present in both training and measurement phases of fingerprinting, constant interference source to a certain level improves the accuracy of fingerprinting, in comparison to the case when no interference is present. Additionally, an increase in the interference power further benefits the fingerprinting accuracy. This is due to the additive influence of interference on the observed RSS values at a certain location, which effectively increases the distance $||e||$ between two training fingerprints, yielding higher KL divergence between two neighboring locations. This result is consistent with the developed theory.

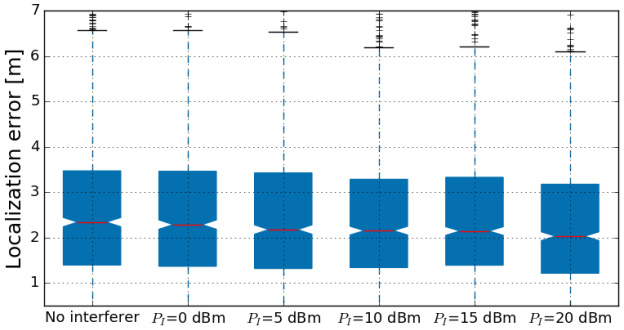

Fig. 6: Influence of the interferer's transmit power in both phases of fingerprinting on the localization accuracy

Supporting the same theoretical claim, if multiple interference sources are introduced in the environment in both phases of fingerprinting, further accuracy improvements can be achieved. This result has been derived through simulation and is depicted in Figure 7. As visible in the figure, introducing additional interferers in the environment (i.e. sequentially Interferer 2, then Interferer 3, then Interferer 4, etc., with their locations as depicted in Figure 5 and with their transmit power set to 10 dBm) yields substantial accuracy improvements. Example-wise, a roughly 20% of average localization error reduction is achieved when 5 interferers are introduced, in contrast to having no interference in the environment.

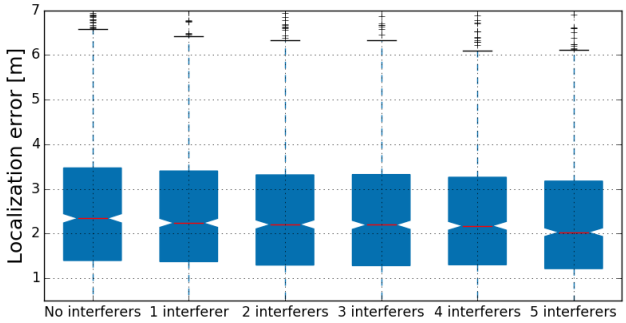

Fig. 7: Influence of the number of interferers in both phases of fingerprinting on the localization accuracy

Next we evaluate the theoretical statement claiming that interference in only one phase of fingerprinting reduces the localization accuracy. Leveraging the same Interferer 1 as previously, but in this case only in the measurement phase of fingerprinting, we observe the localization accuracies as depicted in Figure 8. As visible in the figure, interference in only one phase of fingerprinting (in this case the measurement phase) dramatically reduces fingerprinting accuracy. For example, having only one interferer with constant transmit power of 20 dBm roughly doubles the achieved errors, in comparison to the scenario without interference. These analytically derived results are consistent with the theory, as well as with experimentally obtained indications in the literature ([20], [29]).

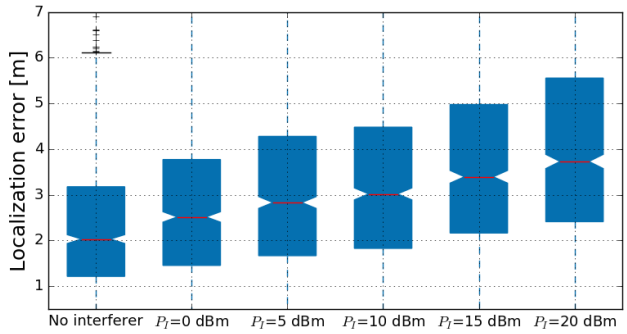

Fig. 8: Influence of the interferer's power in the measurement phase of fingerprinting on the localization accuracy

We further evaluate the theoretical contributions related to the opportunistic selection of localization APs for improving interference robustness of fingerprinting. The theory claims that for improving the system level accuracy of fingerprinting, i.e. its expected accuracy for the whole served environment, a new AP should be positioned as close as possible to the interference source. In our simulation, we again leverage Interfer 1 with its transmit power set to 20 dBm and with its location as indicated in Figure 5. We then introduce a new AP in the served environment, first in the same location as Interferer 1 and later at four random locations in the environment. The achieved localization errors for these scenarios are given in Figure 9. As visible in the figure, introduction of a new AP generally improves fingerprinting accuracy. Furthermore, the highest accuracy improvement of roughly 15% in average

localization error is achieved if a new AP is introduced at the interferer's location. Both results are consistent with the previously developed theory.

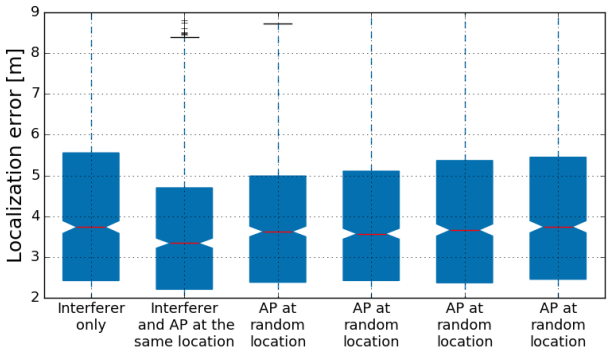

Fig. 9: System level performance vs. location of an additional AP in relation to interferer's location

The theoretically derived results further claim that if the aim is localization of a specific object whose location is vaguely known, then the introduction of a new AP in the vicinity to that object is optimal in terms of fingerprinting accuracy improvement. To evaluate this scenario, we will assume that all our evaluation points are inside of a small square in Figure 5. The location of Interferer 1 is the same as previously. Same as previously, we first introduce a new AP at the same location as Interferer 1. In other scenarios, we introduce a new AP in the vicinity of the small square where the evaluation points are located. This newly introduced AP is labeled with receptively "New AP 1", "New AP 2", "New AP 3", etc., for different scenarios, with their locations as indicated in Figure 5. The localization errors obtained for this set of scenarios are given in Figure 10. As visible in the figure, introducing a new AP at any location in the environment generally improves fingerprinting accuracy. Moreover, introduction of an AP in the vicinity of the evaluation locations yields higher improvement than introducing an AP close to the source of interference. These results are aligned with the respective theory.

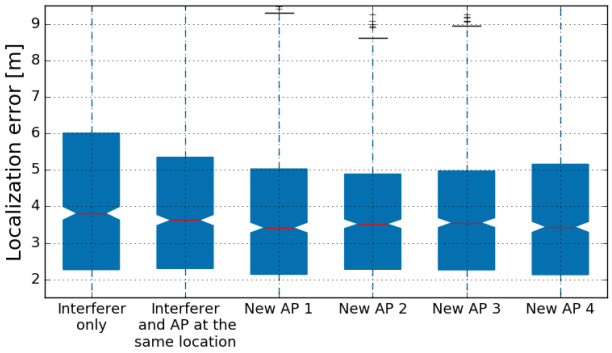

Fig. 10: Performance in a particular area vs. location of an additional AP in relation to interferer's location

B. Experimental Evaluation

We carried the experimental part of the evaluation in the TWIST testbed environment. The evaluation environment is an office building in its usual operation and, at the same time, it is a testbed specifically designed for experimentation focused on the evaluation of indoor localization solutions [30]. In the environment, we generated a training phase by collecting RSS measurements from 4 APs in 32 training points, with their locations as indicated with red dots in Figure 11. The measurements were collected using a specifically designed infrastructure for supporting experimentation related to the evaluation of indoor localization solutions [30]. The infrastructure allows automated, person-less, accurate, and highly repeatable experimentation under controlled and monitored interference conditions. Using the same infrastructure, we further collected 20 measurements in locations labeled with red pins in the figure. These additional 20 measurements were collected in three scenarios, i.e. without interference and with a signal generator as the source of constant interference with two configurations of its transmit power (10 and 20 dBm). The location of the signal generator is indicated in Figure 11. The generated interference was a power envelope of characteristic IEEE 802.11b/g signals without carrier sensing. The interference was generated at the frequency of the APs' operating channel (channel 11), with APs' locations and interference signal spectrum information as depicted in Figure 11.

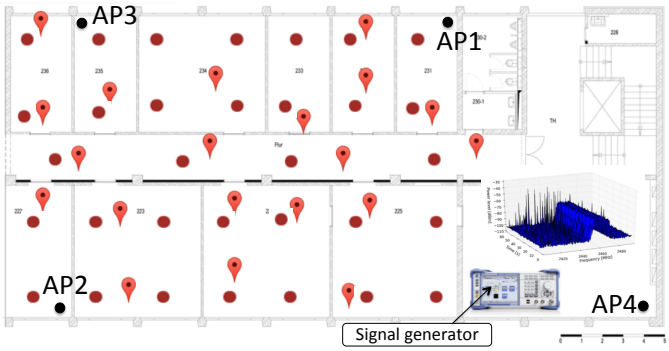

Fig. 11: Locations of APs, training points, evaluation points, and interferer in the testbed environment

We have applied the fingerprinting algorithm on the collected measurements, which yielded 20 estimated locations for each scenario. We further calculated the localization errors for each scenario. The obtained average localization errors per scenario differ substantially, i.e. from 1.94 m in the scenario without interference to 2.67 and 3.31 m in scenarios with interference with interferer's transmit power set to 10 and 20 dBm, respectively. These results are in accordance with the previously derived theory and with the analytically obtained ones. Figure 12 depicts per-point localization errors for different scenarios. As visible in the figure, the evaluation location closer to the source of interference in general experience larger accuracy degradation due to interference being present in the environment. The achieved results support the theoretically derived conclusions, which demonstrates the applicability of the developed theory for modeling the behavior of fingerprinting algorithms under interference in realistic practical conditions.

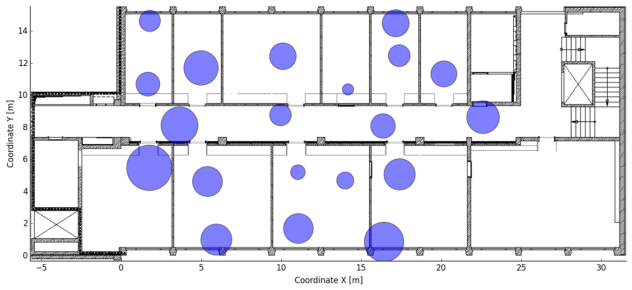

(a) No interference

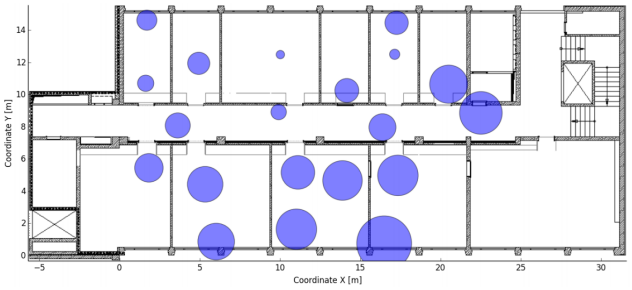

(b) P_I =10 dBm

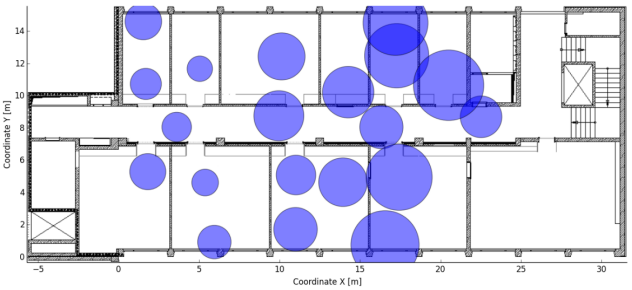

(c) P_I =20 dBm

Fig. 12: Spatial distribution of localization errors in the testbed environment

V. Conclusion

In this work, we characterized the additive effect of interference on the performance of RSSI-based fingerprinting solutions. Our results show the applicability of the previously proposed theoretical framework [18] for modeling interference effect on fingerprinting. Somewhat counterintuitive, we show that interference in both phases of fingerprinting improves its accuracy. Moreover, interference in only one phase degrades the fingerprinting performance. Future work will be oriented toward extending this study to consider the effect of packet loss due to interference on the performance of RSSI-based fingerprinting algorithms.

References

[1] J. G. Andrews, "Interference cancellation for cellular systems: a contemporary overview," *IEEE Wireless Communications*, vol. 12, no. 2, pp. 19–29, 2005.

[2] V. R. Cadambe and S. A. Jafar, "Interference alignment and degrees of freedom of the $ K $-user interference channel," *IEEE Transactions on Information Theory*, vol. 54, no. 8, pp. 3425–3441, 2008.

[3] D. Gesbert *et al.*, "Adaptation, Coordination, and Distributed Resource Allocation in Interference-Limited Wireless Networks," *Proceedings of the IEEE*, vol. 95, no. 12, pp. 2393–2409, 2007.

[4] D. Milioris, G. Tzagkarakis, A. Papakonstantinou, M. Papadopouli, and P. Tsakalides, "Low-dimensional signal-strength fingerprint-based positioning in wireless {lans}," *Ad Hoc Networks*, vol. 12, pp. 100 –114, 2014.

[5] V. Honkavirta *et al.*, "A Comparative Survey of WLAN Location Fingerprinting Methods," in *WPNC 2009*, IEEE, 2009, pp. 243–251.

[6] D. Milioris *et al.*, "Low-Dimensional Signal-Strength Fingerprint-based Positioning in Wireless LANs," *Ad Hoc Networks*, 2011.

[7] C. Laoudias, P. Kemppi, and C. Panayiotou, "Localization using radial basis function networks and signal strength fingerprints in wlan," in *Global Telecommunications Conference, 2009. GLOBECOM 2009. IEEE*, 2009, pp. 1–6.

[8] S. Bai and T. Wu, "Analysis of k-means algorithm on fingerprint based indoor localization system," in *Microwave, Antenna, Propagation and EMC Technologies for Wireless Communications (MAPE)*, 2013, pp. 44–48.

[9] K. Kaemarungsi and P. Krishnamurthy, "Modeling of indoor positioning systems based on location fingerprinting," in *INFOCOM 2004*, vol. 2, 2004, 1012–1022 vol.2.

[10] K. Kaemarungsi, "Efficient design of indoor positioning systems based on location fingerprinting," in *Wireless Networks, Communications and Mobile Computing, 2005 International Conference on*, vol. 1, 2005, 181–186 vol.1.

[11] Y. Wen, X. Tian, X. Wang, and S. Lu, "Fundamental limits of RSS fingerprinting based indoor localization," in *2015 IEEE Conference on Computer Communications (INFOCOM)*, 2015, pp. 2479–2487.

[12] E. Chan, G. Baciu, and S. C. Mak, "Effect of channel interference on indoor wireless local area network positioning," in *Wireless and Mobile Computing, Networking and Communications (WiMob), 2010 IEEE 6th International Conference on*, Oct. Pp. 239–245.

[13] T.-H. Lin, I.-H. Ng, S.-Y. Lau, and P. Huang, "Impact of beacon packet losses to rssi-signature-based indoor localization sensor networks," in *Mobile Data Management: Systems, Services and Middleware, 2009. MDM '09. Tenth International Conference on*, 2009, pp. 389–390.

[14] R. Maheshwari, S. Jain, and S. R. Das, "On estimating joint interference for concurrent packet transmissions in low power wireless networks," in *Proceedings of the Third ACM International Workshop on Wireless Network Testbeds, Experimental Evaluation and Characterization*, ser. WiNTECH '08, New York, NY, USA, 2008, pp. 89–94.

[15] D. Son, B. Krishnamachari, and J. Heidemann, "Experimental study of concurrent transmission in wireless sensor networks," in *Proceedings of the 4th International Conference on Embedded Networked Sensor Systems*, ser. SenSys '06, New York, NY, USA: ACM, 2006, pp. 237–250.

[16] A. Behboodi, N. Wirstrom, F. Lemic, T. Voigt, and A. Wolisz, "Interference effect on localization solutions: signal feature perspective," in *Vehicular Technology Conference (VTC Spring), 2015 IEEE 81st*, IEEE, 2015, pp. 1–7.

[17] A. Behboodi, F. Lemic, and A. Wolisz, "Hypothesis Testing Based Model for Fingerprinting Localization Algorithms," in *2017 IEEE 85th Vehicular Technology Conference (VTC-Spring'17)*, 2017.

[18] A. Behboodi *et al.*, "A Mathematical Model for Fingerprinting-based Localization Algorithms," *arXiv:1610.07636 [cs, math]*, 2016, arXiv: 1610.07636.

[19] D. Tse and P. Viswanath, *Fundamentals of wireless communication*. Cambridge, UK ; New York: Cambridge University Press, 2005, OCLC: ocm57751753.

[20] F. Lemic, A. Behboodi, V. Handziski, and A. Wolisz, "Experimental decomposition of the performance of fingerprinting-based localization algorithms," in *Indoor Positioning and Indoor Navigation (IPIN)*, IEEE, 2014, pp. 355–364.

[21] F. Lemic *et al.*, "Experimental evaluation of rf-based indoor localization algorithms under rf interference," in *Localization and GNSS (ICL-GNSS)*, IEEE, 2015, pp. 1–8.

[22] A. Borrelli, C. Monti, M. Vari, and F. Mazzenga, "Channel models for ieee 802.11 b indoor system design," in *Communications, 2004 IEEE International Conference on*, IEEE, vol. 6, 2004, pp. 3701–3705.

[23] G. Caso *et al.*, "On the applicability of multi-wall multi-floor propagation models to wifi fingerprinting indoor positioning," in *Future Access Enablers of Ubiquitous and Intelligent Infrastructures*, Springer, 2015, pp. 166–172.

[24] F. Lemic *et al.*, "Toward extrapolation of wifi fingerprinting performance across environments," in *Mobile Computing Systems and Applications (HotMobile'16)*, ACM, 2016, pp. 69–74.

[25] F. Lemic, V. Handziski, *et al.*, "Web-based platform for evaluation of rf-based indoor localization algorithms," in *Communication Workshop (ICCW), 2015 IEEE International Conference on*, IEEE, 2015, pp. 834–840.

[26] F. Gustafsson *et al.*, "Mobile positioning using wireless networks: possibilities and fundamental limitations based on available wireless network measurements," *IEEE Signal processing magazine*, vol. 22, no. 4, pp. 41–53, 2005.

[27] G. Mao, *Localization Algorithms and Strategies for Wireless Sensor Networks: Monitoring and Surveillance Techniques for Target Tracking: Monitoring and Surveillance Techniques for Target Tracking*. IGI Global, 2009.

[28] J. Luo and X. Zhan, "Characterization of smart phone received signal strength indication for wlan indoor positioning accuracy improvement," *Journal of Networks*, vol. 9, no. 3, pp. 739–746, 2014.

[29] F. Lemic, A. Behboodi, V. Handziski, and A. Wolisz, "Increasing interference robustness of wifi fingerprinting by leveraging spectrum information," in *Ubiquitous Computing and Communications (IUCC)*, IEEE, 2015, pp. 1200–1208.

[30] F. Lemic, J. Büsch, M. Chwalisz, V. Handziski, and A. Wolisz, "Infrastructure for benchmarking rf-based indoor localization under controlled interference," in *Ubiquitous Positioning Indoor Navigation and Location Based Service (UPINLBS), 2014*, IEEE, 2014, pp. 26–35.